

The stiffness exponent of two-dimensional Ising spin glasses for non-periodic boundary conditions using aspect-ratio scaling

Alexander K. Hartmann,^{1,2,3,*} Alan J. Bray,⁴ A. C. Carter,⁴ M. A. Moore,⁴ and A. P. Young^{1,5}

¹*Department of Physics, University of California, Santa Cruz CA 95064, USA*

²*Ecole Normale Supérieure, 24, Rue Lhomond, 75231 Paris Cedex 05, France*

³*Institut für Theoretische Physik, Universität Göttingen, Bunsenstr.9, 37073 Göttingen, Germany*

⁴*Department of Physics and Astronomy, The University of Manchester, Manchester M13 9PL, UK*

⁵*Theoretical Physics, 1, Keble Road, Oxford OX1 3NP, UK*

(Dated: February 1, 2008)

We study the scaling behavior of domain-wall energies in two-dimensional Ising spin glasses with Gaussian and bimodal distributions of the interactions and different types of boundary conditions. The domain walls are generated by changing the boundary conditions at $T = 0$ in one direction. The ground states of the original and perturbed system are calculated numerically by applying an efficient matching algorithm. Systems of size $L \times M$ with different aspect-ratios $1/8 \leq L/M \leq 64$ are considered. For Gaussian interactions, using the *aspect-ratio scaling* approach, we find a stiffness exponent $\theta = -0.287(4)$, which is independent of the boundary conditions in contrast to earlier results. Furthermore, we find a scaling behavior of the domain-wall energy as predicted by the aspect-ratio approach. Finally, we show that this approach does not work for the bimodal distribution of interactions.

I. INTRODUCTION

Although spin glasses¹ have been studied for more than two decades, finite-dimensional spin glasses are still far from being well understood. This is true also in $d = 2$ dimensions, where no stable spin-glass phase^{2,3,4,5} exists at $T > 0$. The fact that the transition temperature, T_c , is zero can be seen by studying domain walls between ground states induced by changing the boundary conditions. For a system of size $L \times M$, if the domain wall is forced to run in the y -direction, the mean domain-wall energy scales like M^θ in the thermodynamic limit, where θ is the *stiffness exponent*. If $\theta < 0$, as in two-dimensional spin glasses, no stable phase can exist at finite temperature.

Recently⁵ slightly different values of the stiffness exponent have been found for Gaussian distribution of the bonds for different choices of the boundary conditions. Here, by applying the aspect-ratio method⁶, we show that this difference is due to corrections to scaling which persisted, at least for one set of boundary conditions, even for the quite large system sizes used in Ref. 5. The results presented here are consistent with $\theta = -0.287(4)$ for all boundary conditions. This agrees with the result found in Ref. 6 where periodic boundary conditions were applied in all directions for smaller systems than investigated here, indicating a high degree of universality for the exponent θ . Apart from using larger systems and different boundary conditions, we go in another respect beyond the previous work, because aspect ratios, $R \equiv L/M$, less than unity are studied here. This enables us to verify the proposed scaling behavior in the region $R < 1$, where the finite-size scaling depends on the boundary conditions.

The model we study consists of $N = L \times M$ Ising spins

$S_i = \pm 1$ on a square lattice with the Hamiltonian

$$\mathcal{H} = - \sum_{\langle i,j \rangle} J_{ij} S_i S_j, \quad (1)$$

where the sum runs over all pairs of nearest neighbors $\langle i,j \rangle$ and the J_{ij} are quenched random variables. Here, we consider two kinds of disorder distributions:

- (i) Gaussian with zero mean and variance unity,
- (ii) bimodal, i.e. $J_{ij} = \pm 1$ with equal probability.

To study whether an ordered phase is stable at finite temperatures, the following procedure is usually applied^{2,3,4,7}. First a ground state of the system is calculated, having energy E_0 . Then the system is perturbed to introduce a domain wall and the new ground state energy, E_0^{pertb} is evaluated. For each sample, the domain-wall energy is given by $E_{\text{DW}} = |E_0^{\text{pertb}} - E_0|$. Here, we apply free boundary conditions (bc) in the y -direction. To study the scaling behavior of the domain-wall energy, we consider two means to introduce domain walls:

- (i) “P-AP”: First a ground state with periodic bc in the x -direction is calculated. Then the system is perturbed by introducing antiperiodic bc in that directions, e.g. by reversing one line of bonds parallel to the y -direction.
- (ii) “F-DW” (called “F-AF” in Ref. 6): First a ground state with free bc in the x -direction is calculated. For the perturbed system, we then add extra bonds which wrap around the system in the x -direction, and have a sign and strength such that they force the spins they connect to have the opposite relative orientation to that which they had in the original ground state.

In both cases, M denotes the size of the edge along which the boundary conditions are changed to induce a domain wall (i.e. the size in the y -direction). The scaling behavior

$$\langle E_{\text{DW}} \rangle = M^\theta F(L/M) \quad (2)$$

has been predicted⁶, with the following limiting forms:

$$F(R) \sim \begin{cases} R^{-1} & \text{for } R \rightarrow \infty \\ R^{\theta-(d-1)/2} & \text{(P-AP) for } R \rightarrow 0 \\ R^{\theta-(d-1)} & \text{(F-DW) for } R \rightarrow 0. \end{cases} \quad (3)$$

We shall verify that the data does follow this scaling form very well.

II. THE ALGORITHM

In greater than two dimensions, or in the presence of a magnetic field, the exact calculation of spin-glass ground states belongs to the class of NP-hard problems^{8,9}. This means that only algorithms with exponentially increasing running times are known. However, for the special case of a planar system without magnetic field, e.g. a square lattice with periodic boundary conditions in at most one direction, there are efficient polynomial-time “matching” algorithms¹⁰. The basic idea is to represent each realization of the disorder by its frustrated plaquettes¹¹. Pairs of frustrated plaquettes are connected by paths in the lattice and the weight of a path is defined by the sum of the absolute values of the coupling constants which are crossed by the path. A ground state corresponds to the set of paths with minimum total weight, such that each frustrated plaquette is connected to exactly one other frustrated plaquette. This is called a minimum-weight perfect matching. The bonds which are crossed by paths connecting the frustrated plaquettes are unsatisfied in the ground state, and all other bonds are satisfied.

For the calculation of the minimum-weight perfect matching, efficient polynomial-time algorithms are available^{12,13}. Recently, an implementation has been presented¹⁴, where ground-state energies of large systems of size $N \leq 1800^2$ were calculated. Here, an algorithm from the LEDA library¹⁵ has been applied, which limits the system sizes due to the restricted size of the main memory of the computers which we used. Furthermore, each system border with a free boundary decreases the running time relative to a boundary with pbc. The reason is that frustrated plaquettes near a free boundary may be connected even when they are far apart from each other, increasing the number of possible connections. On the other hand, full pcb cannot be realized with the matching algorithm. Hence, we have limited our system sizes to $L \leq 1024, M \leq 16$ for $R \geq 1$, and $L \leq 12, M \leq 768$ for $R < 1$.

III. RESULTS

For Gaussian interactions we have considered systems with P-AP and F-DW boundary conditions with aspect ratios $R = 1/8$ to $R = 64$. We took system sizes $L = 1$ to $L = 12$ for $R = 1/8, 1/4, 1/2$, and $M = 1$ to $M = 16$ for $R = 1, 2, 4, \dots, 64$. Typically $\sim 10^5$ samples were treated per system size (L, M) , except for few combinations, notably $R = 64$ where we studied $\sim 10^4$ samples.

For bimodal interactions we have studied P-AP boundary conditions for $M = 1$ to $M = 16$ ($R = 1, 2, 4, \dots, 64$), with $\sim 10^4$ samples per system size.

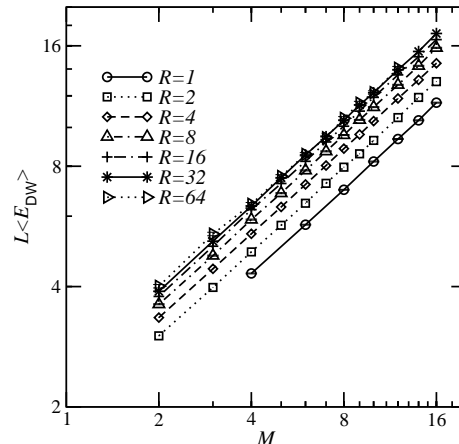


FIG. 1: Average domain-wall energy $\langle E_{\text{DW}} \rangle$ of Gaussian system with P-AP boundary conditions as function of width M for different aspect ratios R . Lines are guides to the eyes only.

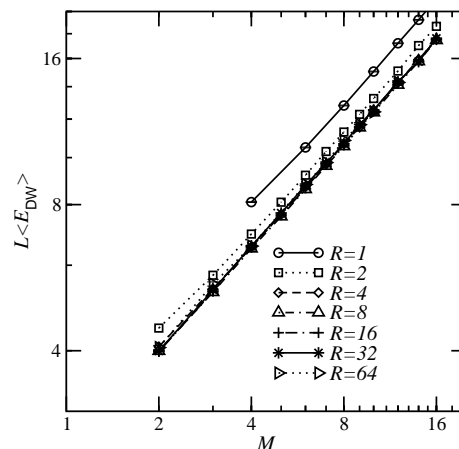


FIG. 2: Average domain-wall energy $\langle E_{\text{DW}} \rangle$ of Gaussian system with F-DW boundary conditions as function of width M for different aspect ratios R . Lines are guides to the eyes only.

We start with the results for the Gaussian distribution. In Figs. 1 and 2 the scaled average domain-wall energies $L\langle E_{\text{DW}} \rangle$ are displayed for P-AP and F-DW boundary conditions respectively. From the scaling theory⁶ a $M^{1+\theta}$

behavior is expected for $R \gg 1$. Indeed for larger values of R and M straight lines are visible in the double logarithmic plot. From fitting to algebraic functions, we have obtained for both cases the values of θ as a function of R ; for small aspect-ratio the small system sizes were omitted from the fits. The results are displayed in Table I.

R	$\theta_{\text{P-AP}}$	$\theta_{\text{F-DW}}$	$\theta_{\text{F-DW}}^{\text{P}}$
1	-0.285(3)	-0.271(2)	-0.153(2)
2	-0.288(3)	-0.279(4)	-0.215(2)
4	-0.288(1)	-0.286(2)	-0.249(2)
8	-0.284(2)	-0.282(2)	-0.265(2)
16	-0.288(2)	-0.284(3)	-0.273(2)
32	-0.289(2)	-0.289(3)	-0.274(3)
64	-0.290(7)	-0.288(7)	

TABLE I: Resulting stiffness exponents from fits to functions $L\langle E_{\text{DW}} \rangle = aM^{1+\theta}$ for P-AP and F-DW boundary conditions. The final column gives the result for F-DW boundary conditions when pbc are applied in the y -direction (data from Ref. 6).

For the P-AP case, the exponent θ is more or less independent of the system size. By contrast, for the F-DW case a significant increase with system size is observed, with the value seeming to converge near the value of the P-AP case for large R . This R -dependence explains why in previous work⁵ ($R = 1$) a difference between P-AP and F-DW has been found. The result found here is compatible with the exponents being equal for both cases. We quote $\theta = -0.287(4)$, which is a conservative estimate including all values of θ found for the P-AP case. This is compatible with the result of $\theta = -0.282(3)$ obtained⁶ for systems with full periodic bc.

Part of the data in Ref. 6 corresponds to the F-DW case with pbc in the y -direction, and we show this here in the final column in Table I, where $M \leq 12$ was used. For this case an even stronger dependence of the effective exponent on R is observed, indicating that corrections to scaling are even larger in this case. We suggest that this is because the pbc forces the domain wall to take at the top and bottom edges the same positions along the x -axis, thereby raising its typical energy. In Ref. 6 it was shown that $\theta_{\text{F-DW}}^{\text{P}}$ (called $\theta_{\text{F-AF}}$ in Ref. 6) nevertheless extrapolates, for $R \rightarrow \infty$, to an asymptotic value consistent with that obtained from the present work, where we employed free boundary conditions in the y -direction.

We have also checked the scaling predictions⁶ for $\langle E_{\text{DW}} \rangle$ explicitly. In Fig. 3 the scaled domain-wall energy $M^{-\theta}\langle E_{\text{DW}} \rangle$ is plotted for all considered values of M as a function of the aspect ratio R . A very good data collapse can be observed (see e.g. right inset of Fig. 3 for P-AP). The functional form of the scaling function agrees very well with the predictions shown in Eq. (3).

In Fig. 4 the normalized standard deviation of the scaling plot is shown as a function of R . Again, the high quality of the scaling can be seen. Note that the statistics for

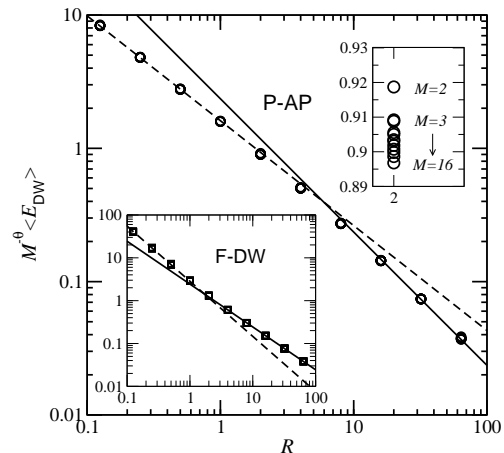


FIG. 3: Scaling plot of $M^{-\theta}\langle E_{\text{DW}} \rangle$, with $\theta = -0.287$, as a function of R for P-AP (main plot) and F-DW (left inset) boundary conditions for all values of M which have been considered. The curve is indeed a (very good) collapse of the results for different values of M , as exemplified for the P-AP case by the right inset, which shows a blow-up of the $R = 2$ points. The lines represent functions $\sim R^{-1}$ (continuous lines), $\sim R^{\theta-(d-1)/2}$ (dashed line, main plot), and $\sim R^{\theta-(d-1)}$ (dashed line, left inset).

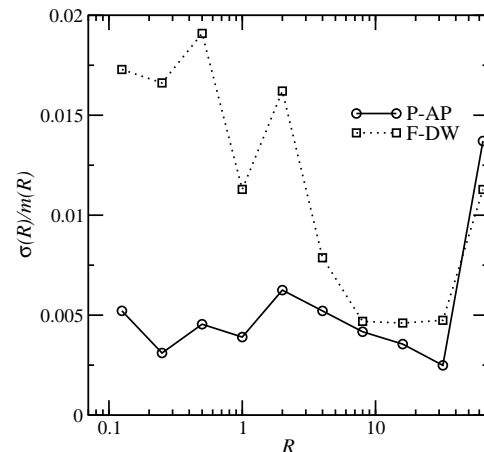


FIG. 4: Standard deviation $\sigma(R)$ of scaling plot points divided by mean $m(R)$. The mean was taken over all considered values of M . Lines are guides to the eyes only.

both P-AP and F-DW cases are comparable, while the statistics for $R = 64$ are worse than for the other values due to the smaller number of samples. From Fig. 4 we see that, for small values of R , the F-DW case scales less well than the P-AP case. This may explain, why, for F-DW, the stiffness exponent obtained for small aspect-ratios differs significantly from the $R \rightarrow \infty$ limit. The fact that F-DW scales less well than P-AP is probably due to the larger influence of the system boundaries induced by the free bc. As a result, the scaling near $R = 1$ is more complicated than a simple $M^{1+\theta}$ behavior.

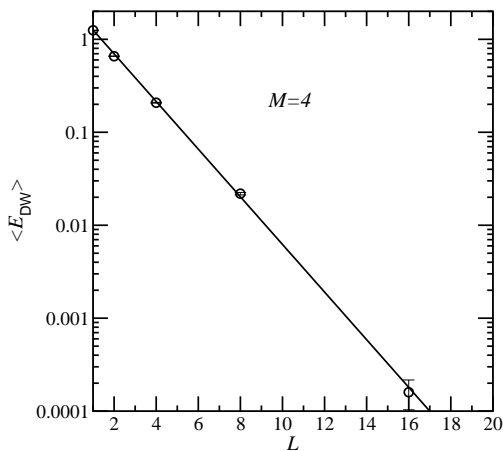


FIG. 5: Domain-wall energy $\langle E_{\text{DW}} \rangle$ of $\pm J$ system with P-AP boundary conditions as a function of L for $M = 4$. The line represents the function $g(L) = 2.27 \exp(-0.59L)$.

Finally, we turn to the system with bimodal distribution of the bonds. In Ref. 5 a saturation of the domain-wall energy has been observed for $R = 1$ when $L = M \rightarrow \infty$, i.e. a fundamentally different result from the Gaussian case. This raises the question of whether the aspect-ratio approach is also able to make those results consistent.

As an example, in Fig. 5 the domain-wall energy is plotted for $M = 4$ as a function of L . Clearly an exponential decrease with L can be observed. This is due to the discrete nature of the interactions and can be explained as follows. For $L \gg M$, the system can be decomposed into almost independent subsystems of size $M \times M$. Let p be the probability to find a *non-zero* domain-wall energy in a subsystem. Then the probability to find a non-zero E_{DW} in the full system is $p^{L/M}$ which decreases exponentially with L .

As a result, for large R (which implies a large value of L for fixed M), the probability to find a non-zero domain-wall energy is so small that for a reasonable number of samples E_{DW} will be exactly zero. This is what we have indeed found for $R = 32$ and $R = 64$. It means that for the bimodal model the aspect-ratio approach cannot be applied. This is in contrast to the Gaussian case, where aspect ratio scaling works better and better with

increasing R .

IV. SUMMARY AND DISCUSSION

We have studied the scaling behavior of the energy of domain walls in two-dimensional spin glasses obtained by changing the boundary conditions at $T = 0$. For the numerical calculations, we have employed a very efficient matching algorithm, enabling us to calculate exact ground states of systems up to size $N = 1024 \times 16$. To eliminate finite-size effects, we have applied the aspect-ratio scaling approach. Our main results are:

- (i) The value of the stiffness exponent for Gaussian distribution of the bonds in $d = 2$ seems to be independent of the choice of the boundary conditions and the way the domain walls are introduced. We give a final value of $\theta = -0.287(4)$.
- (ii) The scaling behavior predicted by the aspect-ratio approach applies very well for the Gaussian distribution of the bonds, again indicating that the value of θ is independent of the boundary conditions.
- (iii) The aspect-ratio technique does *not* allow us to gain further insight for systems with the bimodal distribution of the bonds.

V. ACKNOWLEDGMENTS

The simulations were performed on a Beowulf Cluster at the Institut für Theoretische Physik of the Universität Magdeburg and at the Paderborn Center for Parallel Computing, both in Germany. The main part of the work was done during a visit of AKH to Manchester. Financial support for the visit was provided by the ESF programme SPHINX. AKH also obtained financial support from the DFG (Deutsche Forschungsgemeinschaft) under grants Ha 3169/1-1 and Zi 209/6-1. ACC acknowledges support from EPSRC (UK). APY acknowledges support from the NSF through grant DMR 0086287 and the EPSRC under grant GR/R37869/01. He would also like to thank David Sherrington for hospitality during his stay at Oxford.

* Electronic address: hartmann@theorie.physik.uni-goettingen.de

¹ K. Binder and A.P. Young, Rev. Mod. Phys. **58**, 801 (1986); M. Mezard, G. Parisi, M.A. Virasoro, *Spin glass theory and beyond*, (World Scientific, Singapore 1987); K.H. Fisher and J.A. Hertz, *Spin Glasses*, (Cambridge University Press, Cambridge 1991); A.P. Young (ed.), *Spin glasses and random fields*, (World Scientific, Singapore 1998).

² W.L. McMillan, Phys. Rev. B **30**, 476 (1984).

³ A.J. Bray and M.A. Moore, J. Phys. C **17**, L463 (1984); A.J. Bray and M.A. Moore in *Heidelberg Colloquium on Glassy Dynamics*, J.L. van Hemmen and I. Morgenstern (eds), (Springer-Verlag, Heidelberg 1987).

⁴ H. Rieger, L. Santen, U. Blasum-U, M. Diehl, M. Jünger, and G. Rinaldi, J. Phys. A **29**, 3939-50 (1996).

⁵ A.K. Hartmann and A.P. Young, Phys. Rev B **64**, 180404 (2001)

- ⁶ A.C. Carter, A.J. Bray, and M.A. Moore, Phys. Rev. Lett. **88**, 077201 (2002)
- ⁷ N. Kawashima and H. Rieger, Europhys. Lett. **39**, 85 (1997).
- ⁸ F. Barahona, J. Phys. A **15**, 3241 (1982).
- ⁹ A.K. Hartmann and H. Rieger, *Optimization Algorithms in Physics*, Wiley-VCH, Berlin, to be published 2001.
- ¹⁰ I. Bieche, R. Maynard, R. Rammal, and J.P. Uhry, J. Phys. A **13**, 2553 (1980).
- ¹¹ G. Toulouse, Commun. Phys. **2**, 115 (1977).
- ¹² F. Barahona, R. Maynard, R. Rammal, and J.P. Uhry, J. Phys. A **15**, 673 (1982).
- ¹³ U. Derigs and A. Metz, Math. Prog. **50**, 113 (1991).
- ¹⁴ R.G. Palmer and J. Adler, Int. J. Mod. Phys. C **10**, 667 (1999).
- ¹⁵ K. Mehlhorn and St. Näher, *The LEDA Platform of Combinatorial and Geometric Computing*, Cambridge University Press, Cambridge 1999; see also <http://www.mpi-sb.mpg.de/LEDA/leda.html>.